High-Resolution X-ray Powder Diffraction Studies of Polyethylene and Ethylene−Octene Copolymers: The Setting Angle

M. Lorenzen* and M. Hanfland

European Synchrotron Radiation Facility (ESRF), BP 220, F-38043 Grenoble Cedex, France

Received September 6, 2002; Revised Manuscript Received April 30, 2003

ABSTRACT: The setting angle and the unit cell parameters are investigated for a series of polyethylene samples of crystallinities with compositions between 23% and 75%. Significant variations of the setting angle are observed as a function of crystallinity, melting temperature, and unit cell volume. It is suggested that the setting angle is influenced by defects of the crystal such as folds and incorporated side chains. This conclusion is in agreement with the findings of other authors who studied PE samples of high crystallinities above 67%.

1. Introduction

A large number of studies have been published on the setting angle α of orthorhombic polyethylene (PE) (α is here defined as the angle between the polymer zigzag chain and the *b* axis of the unit cell). Single crystals of PE and highly crystalline PE were investigated (above 67% of crystallinity) either by theoretical methods or by electron, X-ray, or neutron diffraction.

As a result, a large variation of the setting angles was obtained. Therefore, some authors performed systematic studies depending on physical properties. In 1968 Bank et al. predicted a variation of the setting angle with the unit cell volume.[1] However, the verification of his findings was impossible at that time, as studies at very low crystallinities were impossible due to low data quality.[1] Later on, Kawaguchi performed measurements on different PE and paraffin samples and found a variation of the setting angle vs the folding of the molecular chains, imperfections of the crystal lattice, cell dimensions and size of the crystallites.[2] Phillips reported in 1985 that even though systematic studies on the influence of sample properties and thermal history on the unit cell dimensions of PE have been widely studied, an equivalent systematic study is missing in the case of the setting angle.[3] Therefore, he measured the variation of α with the crystallization temperature of pressure-crystallized samples.

According to an analysis of the X-ray powder data published until 1989,[4] only in one study the quality of the data had been good enough to obtain the setting angle with a sufficient accuracy, according to these authors (±2°). To our knowledge no X-ray powder diffraction data for PE have been published ever since. An X-ray fiber study[5] and a theoretical work[6] have been published since then. However, the setting angle remains still a matter of discussion.

We wanted to extend the studied range of crystallinities below the former limit of 67% in order to verify the theoretical prediction described above.[1] Furthermore, the value of the setting angle is important for understanding polyethylene crystallization[4] and dynamics.[7] Therefore, we performed a high resolution X-ray powder diffraction study on a set of six nonoriented PE samples of widely differing crystallinity.

* Corresponding author. E-mail: mlorenzen@online.fr. Fax: (+33) 4 76 88 21 60.

In the following, we present our results comparing them to former data and we discuss the dependence of the setting angle on different properties of the sample.

2. Experimental Section

2.1. Experimental Setup. The experiment was performed on the high-pressure endstation of the beamline ID09 at the European Synchrotron Radiation Facility (ESRF). The X-rays from an undulator-source were focused vertically with a Pt-coated Si mirror and horizontally with an asymmetrically cut bend Si(111) Laue monochromator[8] to a beam size of 30 × 30 μm^2. Diffraction images were collected at a wavelength of 4.6 × 10^{-2} nm. Image plates (size A3) were used as detectors. They were scanned using a Molecular Dynamics STORM image plate reader with 100 μm pixel size. The detector-to-sample distance was 450 mm, leading to a resolution in 2θ of about 0.04°. Both parameters, wavelength and detector-to-sample-distance, were calibrated using a silicon powder pattern. The zero point of the 2θ axis was given by a Gaussian fit of the spot of the attenuated primary beam measured in parallel to each exposure.

2.2. Data Treatment. Spatial distortion, polarisation and detector tilt corrections were performed using the program *fit2d*.[9] One-dimensional diffraction patterns were obtained by integrating the two-dimensional images with the same program.

To resolve the structural parameters of the powder X-ray data, least-squares refinement according to Rietveld is carried out using the program *GSAS*:[10] The carbon positions are refined in the presence of the hydrogen atoms. The distance C−H was fixed to 0.095 nm and the angle H−C−H to 106.1°, as the quality of these X-ray data does not allow the refinement of the hydrogen positions. To fix as few parameters as possible, the C−C bond distances and angles are variable. This allows checking the resulting structural parameters for consistency (see also description of the refinement procedure in refs 4 and 5). The isotropic temperature factors were fixed to the values given by Busing.[5] Other free parameters were the orthorhombic lattice parameters, the non-hydrogen atomic positions, the background coefficients (Chebyschev polynomial), and the scale factor as well as the profile coefficients (multiterm Simpson's rule integration of the pseudo Voigt[10,11]). *GSAS* minimizes the *M* function,[10] and the goodness of the fit is described by χ^2. We get values between $\chi^2 = 3$ and 9.

2.3. Samples. Six different PE samples were studied. Their properties are given in Table 1.

Samples PE1 and PE2 have already been studied by small-angle X-ray scattering under pressure and are described in more detail in ref 13. PE2 is a PE-sample from BASF (Lupolen 1811M) and was heat-treated and calibrated for use as standard in small-angle scattering.[14] More details on PE3 can

10.1021/ma0214411 CCC: $25.00
Published on Web 07/10/2003

Table 1. Properties of the PE Samples[a]

sample	PE 1	PE 2	PE 3	PE 4	PE 5	PE 6
classification	LPE	LDPE	VLDPE	LPE	hEOc	hEOc
T_m (K)	404.7	381.7	398.6	407.1	392.9	377.2
M_w (g/mol)	52 720	75 090	95 000	50 000	51 000	37 000
M_w/M_n	3.87	5.37	4.3	2.8	2.2	2.0
CH_3/1000 C	0	22.97	0	0	0	0
1-octene (mol %)	0	0	5.9	0	2.1	5.2
x_{vc}	0.72	0.40	0.23	0.75	0.61	0.34
ρ (kg/m^3)	958.1	923.4	904	12	12	12

[a] T_m is the melting temperature given as the maximum of the endothermic peak, M_w the weight-averaged molecular weight, M_n the number-averaged molecular weight, x_{vc} the crystalline volume fraction calculated from the enthalpy measured by differential scanning calorimetry (DSC), and ρ the mass density of the bulk sample. The classification has been performed according to ref 18: high-density PE (HPDE), low-density PE (LDPE), very low-density PE (VLDPE), linear PE (LPE), homogeneous ethylene-1-octene copolymer (hEOc).

Table 2. Structural Properties of Orthorhombic PE from the Refinement of the Powder X-ray Diffraction Data[a]

sample	PE 1	PE 2	PE 3	PE 4	PE 5	PE 6
a (nm)	0.741(5)	0.749(3)	0.751(0)	0.742(3)	0.744(6)	0.748(3)
b (nm)	0.494(6)	0.497(4)	0.498(8)	0.494(4)	0.495(5)	0.498(3)
c (nm)	0.255(0)	0.255(0)	0.255(2)	0.254(5)	0.254(7)	0.255(1)
α (deg)	54.4	58.1	60.1	47.8	53.8	58.1
bond distance (nm)	0.1553	0.1542	0.1544	0.1497	0.1483	0.1529
bond angle (deg)	110.5	111.7	111.6	116.4	118.4	113.3
ρ_c (kg/m^3)	996(3)	982(8)	981(1)	997(7)	991(6)	981(7)

[a] The bond distance corresponds to the C−C distance, the bond angle to the C−C−C angle. ρ_c is the density of the crystalline phase as calculated from the structural results.

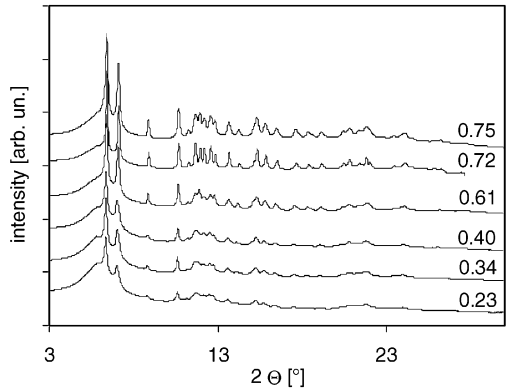

Figure 1. X-ray powder diffraction patterns of the six PE samples. The numbers correspond to the crystallinity.

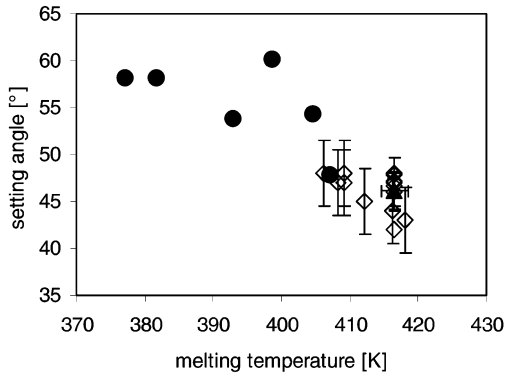

Figure 2. Setting angle vs melting temperature: this work,[19] full circles; experimental data,[3,4,20−23] diamonds; theoretical data,[24] full triangle. Dorset[4] has calculated the standard deviation for the data of Phillips.[3] The value and standard deviation of α calculated theoretically are obtained by averaging the data reported;[6,25−28] the averaged value of the theoretical melting temperature and its standard deviation are taken from ref 29.

be found in ref 15 and on PE4 to PE6 in ref 16 (PE4 is equivalent to JW1114, PE5 to JW1116, and PE6 to JW1120). Furthermore, PE4/JW1114 is described in ref 17.

3. Results

The X-ray powder-diffraction patterns of all samples are shown in Figure 1. The results of the refinement are given in Table 2.

The standard deviation of the setting angle is on the order of 0.02° for all samples. This value is derived from the standard deviation of the lattice parameters *a* and *b* directly given by the refinement program *GSAS* and checked by means of the standard deviations of the observed bond distances and angles of the carbon atoms.

The variations in C−C bond distance and C−C−C bond angle are not significant but are completely due to the errors in the resulting atomic positions. The errors in the lattice parameters are quite small (see Table 2).

4. Discussion

The values obtained for the setting angles α are widely spread (see Table 2). As can be seen by comparing Tables 1 and 2, α varies with the melting temperature and the volume of the orthorhombic unit cell as well as the crystallinity.

4.1. Melting Temperature. As can be seen in Figure 2, the setting angle decreases with increasing melting temperature T_m. T_m is directly related to the thickness of the crystalline lamella l_c. There are different models describing this relation[30] and one is an expression of the form: $T_m(l_c) = T_{mo}[1 - 2\sigma/(\Delta H_m l_c \rho_c)]$ given in Thomson's work,[31] where T_{mo} is the melting temperature for $l_c \rightarrow \infty$, σ the interfacial energy, and ΔH_m the enthalpy of fusion. Thus, the thicker the lamella, the higher the melting temperature. Consequently, the setting angle becomes smaller by increasing the thickness l_c. This is in agreement with former results.[2] Furthermore, the thermal history of the sample (crystallization temperature/pressure and annealing temperature/pressure), the comonomer content and the total degree of branching influence the thickness of the crystalline lamella.[30] High crystallization/annealing temperatures and high crystallization/annealing pressures lead to thicker lamellae. However, the largest

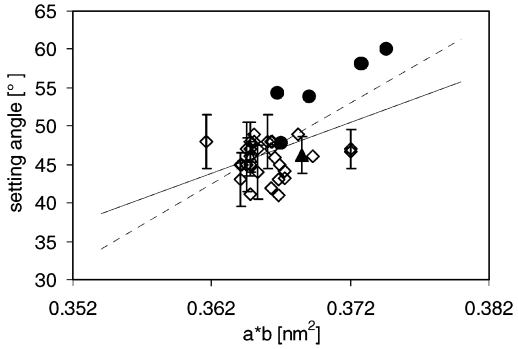

Figure 3. Setting angle vs cross-sectional area a^*b: this work,[32] full circles; experimental data,[1−5,20−23,33−37] diamonds; theoretical value,[6,25−28] full triangle; predicted slope of α^1, full line; fit through all data, dashed line. The predicted slope refers to fully crystalline PE. The standard deviation of the experimental data is displayed whenever given by the authors. The value and standard deviation of α and a^*b of the theoretical data point result from averaging the data reported by the different authors. The standard deviation of 0.21 nm of the theoretical a^*b is so large that it cannot be shown in the graph.

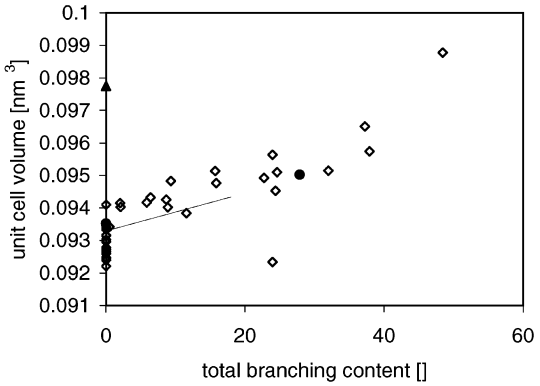

Figure 4. Unit cell volume vs total branching content expressed as amount of side chains per 1000 carbon atoms: this work (PE1, PE2 and PE4), full circles; experimental data,[1−3,35,36,38,41] diamonds; averaged theoretical value,[27,28] full triangle; fit through data of ref 39, line.

attainable thickness is size-limited by the comonomer content and total degree of branching.

However, the lamellar thickness influences not only the setting angle but also the folding, which has been shown on a single crystal and a paraffin sample both having the same lamellar thickness but a different setting angle.[2]

Thus, the setting angle depends on the thermal history as well as on the molecular chain properties.

4.2. Unit Cell Volume. The lattice parameter *c* does not change with respect to the molecular chain properties because it is constrained by the chemical bonds of the molecular chains. Because of the same reason both the linear thermal expansion and compressibility of the *c* axis are negligible in comparison to those of *a* and *b*. Thus, any variation in unit cell volume is equivalent to a variation in the cross-sectional area a^*b.

In Figure 3, the setting angle is shown as a function of a^*b and compared to former results.

As can be seen, the theoretical setting angle matches quite well with the experimental data. However, the theoretical values of the cross-sectional area are quite spread (between 0.346 and 0.413 nm^2). The experimental setting angles increase by increasing the section. Bank et al.[1] stated in 1968 that the setting angle should increase at a rate of 660°/nm^2, basing on the results of their lattice frequency studies in combination with calculations[34] (see full line in Figure 3). The slope of a linear regression through all data points in Figure 3 is 1052°/nm^2. This is a higher slope than predicted by Bank.

The unit cell dimensions *a* and *b* are known to be dependent on branching.[38,39] The larger the branching content the larger the unit cell dimension, owing to incorporation of the branches into the unit cell.[1,38]

This is confirmed by Figure 4, where the unit cell volume is displayed vs the total branching content of all data found in the literature together with the results of this work. As can be seen, the volume is an increasing function of the total branching content.[40]

Other factors could in principle cause the variation of the unit cell dimensions: the way of growing the PE crystal (melt-crystallized, solution grown, or pressure melt-crystallized), quenching and annealing cycles, the kind of solvent, etc.[3,38,42]

It was found, however, that the type of solvent has no influence.[42] No quenching effect could be found either,[38] and the variation due to pressure in pressure melt-crystallized samples is negligible.[3] The influence of the method of growing the crystal remains below 1%.[42]

Different annealing and crystallization temperatures can cause variations of the unit cell volume of up to 1%: [42] the crystals have a larger unit cell volume when the crystallization temperature is lower; the cell volume increases as annealing temperatures increase to about 330 K. Above this value the cell volume decreases. These temperature effects are, however, smaller than the possible effects due to side branches which can amount to about 6% (see Figure 4).

Considering the relationship between α and a^*b shown in Figure 3, it can be argued that the setting angle increases as the degree of branching content increases, as the crystallization temperature decreases and the annealing temperature rises up to 330 K. Furthermore, it diminishes by increasing the annealing temperature above 330 K.

4.3. Crystallinity. The crystallinity expressed as the crystalline volume fraction x_{vc} is another important property characterizing PE samples. x_{vc} can be calculated from either the melting enthalpy[43] or the mass density.[44] Furthermore, it can be estimated from wide- and small-angle scattering.[16,45]

In Figure 5, all literature data found for the setting angle as a function of the crystalline volume fraction are plotted along with our results. Here, the volume fractions are calculated either from mass density or from the melting enthalpy. It is evident that the setting angle decreases as x_{vc} increases. At 100% crystallinity, a value of 45.2° is obtained by a linear regression through all data. It is interesting to notice that a setting angle of 45° was found for $C_{94}H_{190}$, an even-chain orthorhombic paraffin with a lamellar thickness comparable to those of PE.[2]

The crystallinity depends on chain properties (e.g., side chains[16,29]) as well as on the thermal history of the sample.[17]

In Figure 6, the crystalline volume fraction x_{vc} is plotted vs the CH_3 branching content. x_{vc} decreases as the branching content increases due to the difficulties of incorporating the side chains into the crystal. Thus,

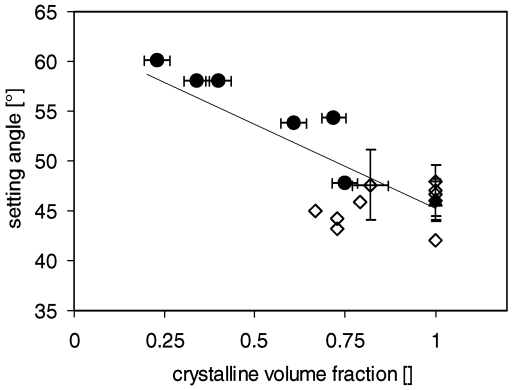

Figure 5. Setting angle vs crystallinity: this work,[19] full circles; experimental data,[1,4,5,20−23,36,46] diamonds; averaged theoretical value,[25,26,28] full triangle; fit through all data, line.

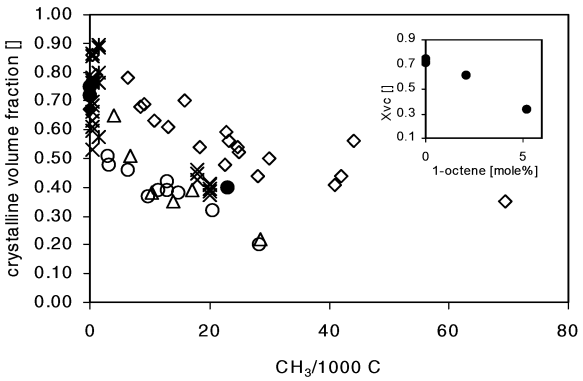

Figure 6. Crystalline volume fraction data vs CH_3 branching content (inset: crystalline volume fraction data vs 1-octene-branching content): this work, full circles; ref 29, empty diamonds; ref 36, full diamonds; ref 41, triangles; ref 45, crosses; ref 47, circles; ref 48, stars.

the setting angle is a decreasing function of the side-branching content, as already stated in the last section.

The differences between the data on CH_3 branching content of the various authors in Figure 6 could be explained in terms of thermal history, of chain properties other than branching (e.g., molecular weight), of systematic differences in the estimation of crystallinity, and in terms of additional side branches of other types which incorporate to a different extent into the crystal.

The influence of the thermal history on the crystallinity of PE has been widely studied. Roughly speaking, the crystallinity increases as the crystallization pressure and temperature as well as the annealing temperature increase.[49] Cooling rates and time spent at fixed temperature play an important role.

From the systematic study of Kortleve,[45] it can be estimated that cooling rate and CH_3-side-branching content influence the crystallinity of PE samples to roughly the same extent.

Phillips studied the change in setting angle as a function of the crystallization pressure.[3] He stated a decrease in α by increasing crystallization pressure. This is in agreement with our results as the crystallinity increases with increasing pressure.

5. Summary

To summarize, relationships between α and different macroscopic properties such as crystallinity and melting temperature as well as microscopic properties such as unit cell volume and chain branching could be stated. They are discussed within the known relationships between macroscopic and microscopic properties as well as the thermal history of the sample. It is known that the setting angle is not a constant (e.g. refs 1 and 2). However, this was not yet studied on a large variety of different samples. In particular, the region of low crystallinity has not been explored so far, and for the first time, values below 67% down to even 23% are reported.

Acknowledgment. We would like to thank H. Reynaers and B. Goderis from the University of Leuven, Belgium, for the samples PE3-PE6 and fruitful discussions as well as the ID02 team at the ESRF for the sample PE2.

References and Notes

(1) Bank, M. I.; Krimm, S. *J. Appl. Phys.* **1968**, *39*, 4951−4958.
(2) Kawaguchi, A.; Ohara, M.; Kobayashi, K. *J. Macromol. Sci.—Phys.* **1979**, *B16*, 193−212.
(3) Phillips, P. J.; Tseng, H. T. *Polymer* **1985**, *26*, 650−654.
(4) Dorset, D. L. *Polymer* **1986**, *27*, 1349−1352.
(5) Busing, W. R. *Macromolecules* **1990**, *23*, 4608−4610.
(6) Boyle, A. *J. Mol. Graphics* **1994**, *12*, 219−225.
(7) Twisleton, J. F.; White, J. W. In *Neutron Inelastic Scattering*; International Atomic Energy Agency: Vienna, 1972; p 301.
(8) Schulze, C.; Lienert, U.; Hanfland, M.; Lorenzen, M.; Zontone, F. *J. Synchrotron Radiat.* **1998**, *5*, 77−81.
(9) Hammersley, A. P.; Svensson, S. O.; Hanfland, M.; Fitch, A. N.; Häusermann, D. *High-Pressure Res.* **1996**, *14*, 235−248.
(10) Larson, A. C.; von Dreele, R. B. *GSAS− General Structure Analysis System*; Los Alamos National Laboratory, LAUR: Los Alamos, NM, 86−748.
(11) Howard, C. J. *J. Appl. Phys.* **1982**, *15*, 615−620.
(12) Samples PE4 to PE6 are quite porous and, thus, include a lot of air. Therefore, the density cannot be measured with standard methods.
(13) Lorenzen, M.; Bösecke, P.; Ferrero, C.; Riekel, C.; Eichler, A. *Macromolecules* **1997**, *30*, 6645−6649.
(14) Zemb, T. Saclay, Gif-sur-Yvette, France. Personal communication.
(15) Deblieck, R. A. C.; Mathot, V. B. F. *J. Mater. Sci. Lett.* **1988**, *7*, 1276−1280.
(16) Goderis, B. *Morphology and crystallinity of linear low-density polyethylene*, Diploma work, Katholik University of Leuwen, 1993.
(17) Vanden Eynde, S.; Mathot, V. B. F.; Koch, M. H. J.; Reynaers, H. *Polymer* **2000**, *41*, 4889−4900.
(18) Mathod, V. B. F.; Scherrenberg, R. L.; Pijpers, T. F. J. *Polymer* **1998**, *39*, 4541−4559.
(19) The error bars in α are smaller than the sign.
(20) Kawaguchi, A. *Polymer* **1981**, *22*, 753−761.
(21) Hu, H.; Dorset, D. L. *Acta Crystallogr.* **1989**, *B45*, 283−290.
(22) Dorset, D. L. *Macromolecules* **1991**, *24*, 1175−1178.
(23) Ogawa, D.; Moriguchi, S.; Isoda, S.; Kobayashi, T. *Polymer* **1994**, *35*, 1132−1136.
(24) The theoretical data refer to fully crystalline PE.
(25) Williams, D. E. *J. Chem. Phys.* **1967**, *47*, 4680−4684.
(26) Boyd, R. H. *J. Polym. Sci., Polym. Phys. Ed.* **1975**, *13*, 2345.
(27) Grossmann, H. P.; Frank, W. *Polymer* **1977**, *18*, 341−344.
(28) Davé, R. S.; Farmer, B. L. *Polymer* **1988**, *29*, 1544−1554.
(29) Quirk, R. P.; Alsamarraie, M. A. A. In *Polymer Handbook*, 3rd ed.; Brandrup, J., Immergut, E. H., Eds.; John Wiley and Sons: New York, 1989; p V/15.
(30) Magill, J. H. In *Polymer Handbook*, 3rd ed.; Brandrup, J., Immergut, E. H., Eds.; John Wiley and Sons: New York, 1989; p VI/279.
(31) Hoffmann, M.; Krömer, H.; Kuhn, R. *Polymeranalytik I*; Georg Thieme Verlag: Stuttgart, Germany, 1977.
(32) The error bars in both directions are smaller than the sign.
(33) Bunn, C. W. *Trans. Faraday Soc.* **1939**, *35*, 482−491.
(34) Tasumi, M.; Krimm, S. *J. Chem. Phys.* **1967**, *46*, 755−766.
(35) Kasai, A.; Kakudo, M. *Rep. Prog. Polym. Phys. Jpn.* **1968**, *11*, 145−148.
(36) Kavesh, S.; Schultz, J. M. *J. Polym. Sci. Part A-2* **1970**, *8*, 243−276.
(37) Wunderlich, B. *Crystal Structure, Morphology, Defects*; Academic Press: New York, 1973.
(38) Swan, P. R. *J. Polym. Sci.* **1962**, *56*, 409−416.

(39) Alizadeh, A.; Muñoz-Escalona, A.; Vallejo, B.; Martínez-Salazar, J. *Polymer* **1997**, *38*, 1207−1214.
(40) It is interesting to notice that the volume-branching relationship is independent of the type of side branches (compare with ref 38).
(41) Schouterden, P.; Vandermaliere, M.; Riekel, C.; Koch, M. H. J.; Groeninckx, G.; Reynaers, H. *Macromolecules* **1989**, *22*, 237−244.
(42) Davis, G. T.; Eby, R. K.; Martin, G. M. *J. Appl. Phys.* **1968**, *39*, 4973−4980.
(43) The melting enthalpy can be measured by DSC. The melting enthalpy of 100% crystalline PE serves as reference (0.293 J/kg).
(44) $x_{vc} = (\rho - \rho_a)/(\rho_c - \rho_a)$, where ρ is the sample density, $\rho_a = 855$ kg/m^3 is the amorphous density, and $\rho_c = 1000$ kg/m^3 is the crystalline density.
(45) Kortleve, G.; Vonk, C. G. *Kolloid-Z. Z. Polym.* **1968**, *225*, 124−131.
(46) Hikosaka, M.; Seto, T.; Minomura, S. *Polym. Prepr. Jpn.* **1977**, *26*, 421.
(47) Defoor, F. Molecular thermal and morphological characterization of narrowly branched fractions of 1-Octene linear low-density polyethylene. Ph.D. Thesis, Katholik University of Leuwen, 1992.
(48) Davis, G. T.; Eby, R. K.; Colson, J. P. *J. Appl. Phys.* **1970**, *41*, 4316−4326.
(49) Zachmann, H. G. In *Physik der Kunststoffe* In *Kunststoff-Handbuch*; Vieweg, R., Braun, D., Eds.; Carl Hanser Verlag: München, 1975; Vol. 1.

MA0214411